DNA Binding Studies of a New Dicationic Porphyrin. Insights into Interligand Interactions†

Alexander H. Shelton,‡ Alison Rodger,§ and David R. McMillin*,‡

Department of Chemistry, 560 Oval Drive, Purdue University, West Lafayette, Indiana 47907-2084, and Department of Chemistry, University of Warwick, Coventry CV4 7AL, U.K.

Received February 10, 2007; Revised Manuscript Received May 17, 2007

ABSTRACT: Cationic porphyrins have an affinity for DNA and potential for applications in the fields of photodynamic therapy and cellular imaging. This report describes a new dicationic porphyrin, 5,15-dimethyl-10,20-di(*N*-methylpyridinium-4-yl)porphyrin, abbreviated H_2tMe_2D4. Although tetrasubstituted, H_2tMe_2-D4 presents modest steric requirements and forms in reasonable yield by a "2+2" synthetic method. Accordingly, studies of the zinc(II)- and copper(II)-containing derivatives, Zn(tMe_2D4) and Cu(tMe_2D4), have also been possible. Methods used to characterize DNA-binding motifs include absorption, emission, linear, and circular dichroism spectroscopies, as well as viscometry. An unusually detailed picture of porphyrin uptake emerges. As the ratio of DNA to porphyrin increases during a typical titration, H_2tMe_2-D4 or Cu(tMe_2D4) initially aggregates on the host and then shifts to intercalative binding at close quarters before finally dispersing into non-interacting intercalation sites of the host. Emission studies of the copper(II) porphyrin have been very valuable. The existence of a measurable signal is diagnostic of intercalative binding, and the saturation behavior establishes that internalization typically monopolizes approximately three base pairs. In the moderate loading regime, emission data are most telling because dipole−dipole interactions between near-neighbor porphyrins tend to confuse other spectroscopic assays. The third ligand, Zn(tMe_2D4), behaves differently in that the uptake is a strictly cooperative process. The mode of binding also varies with the base content of the DNA host. When the DNA is rich in A=T base pairs, the porphyrin remains five-coordinate and binds externally; however, Zn(tMe_2D4) loses its axial ligand and binds by intercalation if the host contains only G≡C base pairs.

Water-soluble, cationic porphyrins are useful as chemical and spectroscopic probes of DNA structure (*1*−*4*). They also offer promise for various therapeutic applications, e.g., as sensitizers for photodynamic therapy (*5*, *6*), antibacterial agents (*7*), or inhibitors of teleomerase (*8*), an enzyme that plays a key role in extending the lifetime of tumor cells (*9*). Early work by Fiel and co-workers on 5,10,15,20-tetra(*N*-methylpyridinium-4-yl)porphyrin (H_2T4[1] in Scheme 1) stimulated many subsequent studies (*10*, *11*). As discussed in the reviews already cited (*1*−*4*), the consensus view is that H_2-T4 or one of its derivatives interacts with a particular B-form DNA duplex by one of three limiting binding motifs: intercalation between base pairs, external (groove) binding, or aggregation on the surface of the DNA macromolecule. Cooperative binding interactions can also occur. Many factors influence adduct formation, and one of the most important considerations is the composition of the DNA host. The empirical findings are that the presence of adenine·thymine (A=T) base pairs promotes external binding of H_2T4, while intercalation is more likely to occur within sequences that are rich in guanine·cytosine (G≡C) base pairs (*12*−*16*). The likely explanation is that the structural reorganization required for formation of a high-affinity external binding pocket is simply more feasible in a low-melting region of DNA, i.e., one that is rich in A=T base pairs (*17*−*19*). On the other hand, more rigid runs of DNA, which are rich in G≡C base pairs, tend to *disfavor* external binding and promote intercalative binding (*18*, *20*, *21*). The ionic strength of the solution is another important factor that influences binding. At lower ionic strengths, intercalative binding tends to be more favored (*22*, *23*), while external binding or even assembly of the porphyrin on the surface of the DNA surface becomes more favorable at higher ionic strengths (*24*).

Steric considerations are also important. The most obvious steric problems arise outside the plane of the porphyrin. Thus, axially ligated metalloporphyrins cannot intercalate between base pairs (*25*). Intercalation is apparently also impossible

† This work was supported by grants from the Engineering and Physical Sciences Research Council (GR/T09224/01 to A.R.) and the National Science Foundation (CHE-0550241 to D.R.M.).

* To whom correspondence should be addressed. E-mail: mcmillin@purdue.edu. Fax: (765) 494-0239. Phone: (765) 494-5452.

‡ Purdue University.

§ University of Warwick.

[1] Abbreviations: $H_2(tMe_2D4)$, 5,15-dimethyl-10,20-di(*N*-methylpyridinium-4-yl)porphyrin; Zn(tMe_2D4), [5,15-dimethyl-10,20-di(*N*-methylpyridinium-4-yl)porphyrinato]zinc(II); Cu(tMe_2D4), [5,15-dimethyl-10,20-di(*N*-methylpyridinium-4-yl)porphyrinato]copper(II); CD, circular dichroism; H_2T4, 5,10,15,20-tetra(*N*-methylpyridinium-4-yl)porphyrin; CuT4, [5,10,15,20-tetra(*N*-methylpyridinium-4-yl)porphyrinato]copper(II); H_2D4, 5,15-di(*N*-methylpyridinium-4-yl)porphyrin; H_2D3, 5,15-di(*N*-methylpyridinium-3-yl)porphyrin; H_2T_{agg}, 5,15-diphenyl-10,20-di(*N*-methylpyridinium-4-yl)porphyrin; DCM, dichloromethane; DMF, *N*,*N*-dimethylformamide; $CDCl_3$, deuterated chloroform; 5-Me-DPM, 5-methyldipyrromethane; H_2D4n, 5,15-di(4-pyridyl)porphyrin; H_2tMe_2-D4n, 5,15-dimethyl-10,20-di(4-pyridyl)porphyrin; bp, base pairs; LD, linear dichroism; LD^r, reduced linear dichroism; SRV, standard reduced viscosity ratio; *q*, base pair-to-porphyrin ratio; *R*, porphyrin-to-base pair ratio.

10.1021/bi700293g CCC: $37.00
Published on Web 07/14/2007

Scheme 1

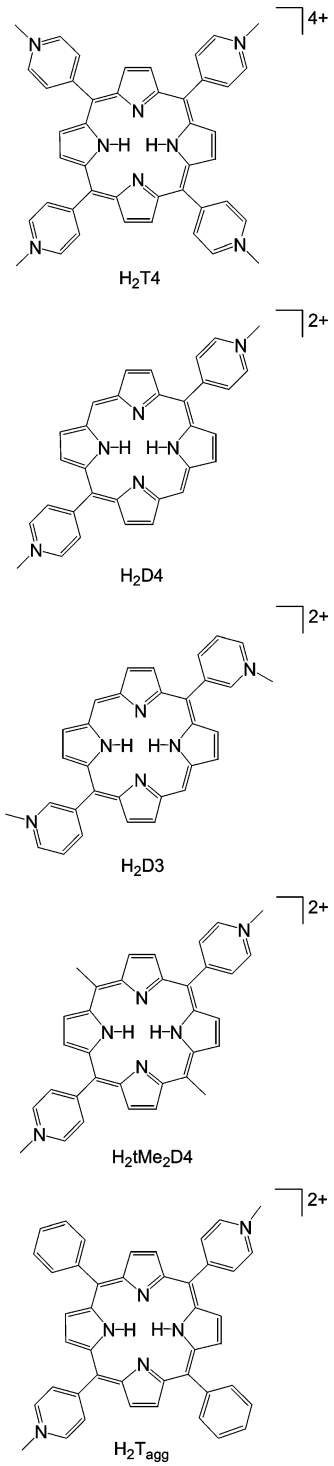

for porphyrins carrying too many *N*-methylpyridinium-2-yl groups (*23*). Other steric interactions are also possible, and the sheer size of a substituent like the *N*-methylpyridinium ion, whether the linkage is via its C2, C3, or C4 position, has long been recognized as a likely influence on DNA binding interactions (*11*). Williams and co-workers provided some insight when they determined the crystal structure of a DNA duplex combined with Cu(T4), the copper(II)-containing derivative of H_2T4 (*26*). The structure showed that fraying occurred at the end of the helices, and the conclusion was that fraying occurs because significant steric clashes occur within the minor groove where *N*-methylpyridinium-4-yl groups of the intercalator impinge on the sugar−phosphate backbone of DNA. In a subsequent study, Guliaev and Leontis used ^{1}H NMR methods to determine the structure of an intercalated form of H_2T4 in solution; however, they did not report any particular steric problems (*27*). The latter study raises the possibility that the end fraying effect is a packing-induced artifact that occurs in the solid state. To address the issue experimentally, the McMillin group synthesized the sterically less demanding porphyrins 5,15-di(*N*-methylpyridinium-4-yl)porphyrin and 5,15-di(*N*-methylpyridinium-3-yl)porphyrin, denoted H_2D4 and H_2D3, respectively, in Scheme 1 (*18*, *28*). Note that the latter porphyrins need to insert only one *N*-methylpyridiniumyl substituent into the minor groove to intercalate into B-form DNA. Consistent with the idea that the steric bulk of H_2T4 inhibits intercalation in certain domains, H_2D4 and H_2D3 both act as universal intercalators (*18*, *28*). In other words, both porphyrins bind as intercalators, regardless of the base composition of the DNA host.

Unfortunately, progress in the area of sterically less demanding porphyrins has been slow. One reason is a materials limitation in that the synthetic yields reported for the H_2D4 and H_2D3 derivatives are very low. Studies are also time intensive because characterization of an adduct usually depends upon the application of an array of physical methods, most often absorption spectroscopy, circular dichroism (CD), and viscometry (*3*, *4*). Furthermore, the nature of the adduct may change with conditions, e.g., the extent of loading. The investigation reported below addresses these problems and describes a promising new porphyrin, 5,15-dimethyl-10,20-di(*N*-methylpyridinium-4-yl)porphryin, denoted herein as H_2tMe$_2$D4 (Scheme 1). The relative ease of preparation has made possible the extension of studies to include the copper(II) and zinc(II) derivatives, Cu(tMe$_2$D4) and Zn(tMe$_2$D4), respectively. The H_2tMe$_2$D4 system also makes an interesting contrast with 5,15-diphenyl-10,20-di(*N*-methylpyridinium-4-yl)porphyrin, or H_2T_{agg} in Scheme 1, a formally related porphyrin that is exceptionally prone to assembling on the DNA surface (*25*, *29*). The less hydrophobic H_2tMe$_2$D4 porphyrin is generally less prone to aggregation; however, Cu(tMe$_2$D4) has a tendency to aggregate in solution, and near-neighbor interactions occur for other H_2tMe$_2$D4 species under conditions of high drug loading. The luminescence properties of Cu(tMe$_2$D4) provide unique insight into adducts present in the high-loading regime where ligand−ligand interactions are inevitable. While H_2tMe$_2$D4 and Cu(tMe$_2$D4) behave as universal intercalators, the uptake of Zn(tMe$_2$D4) proves to be a base-dependent, strictly cooperative process.

EXPERIMENTAL PROCEDURES

Materials

Sigma-Aldrich sold 2-acetylpyrrole, 4-pyridinecarboxaldehyde, acetaldehyde, boron trifluoride diethyl etherate, copper acetate, dichlorodimethylsilane, florisil, methyl-*p*-toluenesulfonate, potassium hexafluorophosphate, sodium borohydride, tetrabutylammonium nitrate, Trizma base, Trizma HCl, and aluminum-backed silica gel thin layer chromatography plates with a fluorescent indicator. Pyrrole came from either Lancaster Synthesis or Acros Organics. Acetic anhydride, acetone, acetonitrile, ammonium hydrox-

ide, chloroform, dichloromethane (DCM), ether, ethyl acetate, glacial acetic acid, hexane, hydrochloric acid, methanol, *N*,*N*-dimethylformamide (DMF), potassium carbonate, potassium nitrate, silica gel, sodium carbonate, sodium hydroxide, sodium sulfate, and zinc acetate were products from Fisher or Mallinckrodt. Deuterated chloroform ($CDCl_3$) was from Sigma-Aldrich or Cambridge Isotope Labs. GE Healthcare (formally Amersham Biosciences) supplied sonicated salmon testes DNA (ST DNA) and poly(deoxyguanylic-deoxycytidylic) acid sodium salt {[poly(dG-dC)]$_2$}, while the poly(deoxyadenylic-deoxythymidylic) acid sodium salt {[poly(dA-dT)]$_2$} was from Midland Certified Reagent Company, Inc. The micron filters (0.22, 0.45, and 0.6 μm) were from Millipore Corp. or Pall Corp. Except as noted, commercial chemicals saw no purification. However, the deionized water did pass through a Barnstead Bantam water purification system with a mixed-bed cartridge.

Synthetic Procedures

Various literature reports helped shape the approaches taken for the synthesis of 2-(1-hydroxyethyl)pyrrole (*30*), 5-methyldipyrromethane (*30*), and 5,15-dimethyl-10,20-di(pyrid-4-yl)porphyrin (*18*, *23*, *31*, *32*).

2-(1-Hydroxyethyl)pyrrole. Rapid stirring induced 2-acetylpyrrole (25 g, 0.229 mol) to dissolve in a mixture of diethyl ether (229 mL) and water (678 mL). After the addition of sodium borohydride (34.652 g, 0.916 mol) in water (229 mL), the mixture was stirred for 48 h while reduction occurred. Subsequent steps involved extraction into ether and drying with sodium sulfate. After the drying agent had been filtered off, evaporation of the ether yielded the desired alcohol as an oil (84%): ^{1}H NMR ($CDCl_3$) δ 1.48 (d, 3H), 2.56 (s, 1H), 4.79 (m, 1H), 6.02 (s, 1H), 6.11 (q, 1H), 6.67 (d, 1H), 8.77 (s, 1H).

5-Methyldipyrromethane (5-Me-DPM). The reaction proceeded during dropwise (over the period of 1 h) addition of 9 g (0.081 mol) of 2-(1-hydroxyethyl)pyrrole to a flask containing 1.0 mL (8.1 mmol) of boron trifluoride diethyl etherate and 112.4 mL (1.62 mol) of pyrrole. The reaction time was 12 h with stirring under a nitrogen atmosphere. Subsequent workup involved the addition of 200 mL of dichloromethane and three washes with aqueous solutions containing 0.05 M sodium hydroxide and 10% (by mass) sodium carbonate. After drying over sodium sulfate, the organic layer yielded a dark viscous oil. After two extractions from florisil in conjunction with hexane and a Soxhlet extractor, a pale yellow solid slowly formed as the hexane evaporated (56% yield): ^{1}H NMR ($CDCl_3$) δ 1.70 (d, 3H), 4.30 (q, 1H), 6.17 (s, 2H), 6.25 (q, 2H), 6.76 (q, 2H), 7.96 (broad s, 1H).

5,15-Dimethyl-10,20-di(pyrid-4-yl)porphyrin (H_2tMe$_2$D4n). The reaction flask usually contained glacial acetic acid (300 mL), acetic anhydride (30 mL), and 4-pyridinecarboxaldehyde (0.42 mL, 4.2 mmol). The addition of the other component, 5-Me-DPM, occurred in portions and involved addition of aliquots of a 5 mL solution in glacial acetic acid prior to each of a series of heating steps. The heating times increased from 45 s to 2 min for reaction in a microwave oven under air. The cooling time was 30 min after each heating step. The workup steps include evaporation of the acid medium, dissolution in dichloromethane, filtration, and extraction with an aqueous base. Successive elutions from florisil with 2% methanol in DCM gave the desired porphyrin. The last purification step involved crystallization from an 8% dichloromethane/methanol solvent system. The final product deposited as a shiny purple amorphous solid (ca. 4% yield): calcd for $C_{32}H_{24}N_6 \cdot 1.5H_2O$ 73.98% C, 5.23% H, 16.17% N, found 74.19% C, 5.05% H, 16.00% N; ^{1}H NMR ($CDCl_3$) δ −2.64 (s, 2H), 4.64 (s, 6H), 8.14 (d, 4H), 8.82 (d, 4H), 9.05 (d, 4H), 9.51 (d, 4H); CI-MS ($C_{32}H_{24}N_6$) 492; $\epsilon_{416.5}$ (DCM) = 312 000 M^{-1} cm^{-1}.

[5,15-Dimethyl-10,20-di(N-methylpyridinium-4-yl)porphyrin](p-toluenylsulfonate)$_2$·H_2O. A modified literature method was used to methylate the neutral dipyridyl porphyrin (*18*). In addition to DMF as a solvent and methyl *p*-toluenesulfonate as the methylating agent, the reaction solution contained potassium carbonate. The reaction temperature was 60 °C under an atmosphere of nitrogen. It was convenient to follow the course of the reaction by a TLC method (*33*). After filtration, addition of a soluble nitrate salt induced precipitation of the product. Purification involved dissolution in water and treatment with dilute hydrochloric acid. Dropwise addition of aqueous potassium hexafluorophosphate induced precipitation of the red/brown hexafluorophosphate salt. Conversion to the nitrate salt was possible by a metathesis procedure: calcd for $C_{48}H_{44}N_6O_6S_2 \cdot H_2O$ 65.30% C, 5.25% H, 9.52% N, found 65.28% C, 5.42% H, 9.58% N; MALDI-MS ($C_{32}H_{24}N_6$) 522.2; ^{1}H NMR (DMSO-d_6) δ −3.62 (s, 2H), 3.88 (s, 6H), 3.92 (s, 6H), 8.17 (d, 4H), 8.20 (d, 4H), 8.65 (d, 4H), 9.11 (d, 4H).

{[5,15-Dimethyl-10,20-(N-methylpyridinium-4-yl)porphyrinato]Zn(II)}(NO_3)$_2$·0.5H_2O. The preparation involved the combination of H_2tMe$_2$D4 (59.9 mg, 92.7 μmol) with zinc acetate (148.0 mg, 927.0 μmol) in water and heating to 60 °C under nitrogen. After the reaction was over and the solution cooled to room temperature, the product deposited on addition of an aqueous solution of potassium hexafluorophosphate. A subsequent metathesis procedure then yielded the nitrate salt: calcd for $C_{34}H_{28}N_8O_6Zn \cdot 0.5H_2O$ 56.80% C, 4.06% H, 15.58% N, found 57.24% C, 4.13% H, 15.32% N.

{[5,15-Dimethyl-10,20-(N-methylpyridinium-4-yl)porphyrinato]Cu(II)}(PF_6)$_2$·0.5H_2O. The reaction was similar to that for the incorporation of zinc except that the solvent was DMF. Addition of tetrabutylammonium nitrate induced precipitation of the complex from DMF, and a metatheis procedure yielded the hexafluorophosphate salt: calcd for $C_{34}H_{28}N_6P_2F_{12}Cu \cdot 0.5H_2O$ 46.24% C, 3.31% H, 9.52% N, found 45.93% C, 3.38% H, 9.24% N.

Methods

Silanization of the cuvettes and other selected glassware helped minimize adsorption of the cationic porphyrins during spectral studies (*34*). The extinction coefficients used for concentration determinations were as follows: ϵ_{260} = 13 600 M^{-1} cm^{-1} for [poly(dA-dT)]$_2$ (*35*), ϵ_{254} = 16 800 M^{-1} cm^{-1} for [poly(dG-dC)]$_2$ (*36*), and ϵ_{260} = 13 200 M^{-1} cm^{-1} for ST DNA (*37*), all in units of base pairs. Beer's law plots yielded the following in Tris buffer (pH 7.50, μ = 0.05 M): $\epsilon_{416.5}$ = 190 000 M^{-1} cm^{-1} for H_2tMe$_2$D4, $\epsilon_{418.5}$ = 170 000 M^{-1} cm^{-1} for Cu(tMe$_2$D4), and ϵ_{428} = 150 000 M^{-1} cm^{-1} for Zn(tMe$_2$D4). The solvent used for determination of the

extinction coefficient for the copper analogue was 1:1 methanol/Tris buffer (pH 7.50, $\mu = 0.05$ M).

The buffer for the DNA binding studies was a $\mu = 0.05$ M, pH 7.50 Tris buffer. The porphyrin concentration was typically 1.7 μM for spectrophotometric investigations. The calculated %H, or hypochromic response, represents the percent drop in absorbance at the Soret maximum due to formation of an adduct with DNA. For quantifying all spectral *changes* associated with adduct formation, the reference was usually free porphyrin in Tris buffer. The exception was the hypochromism associated with the binding of Cu(tMe_2D4), in which case the reference solution was 50% MeOH, to ensure comparison with a monomeric form, vida infra. During luminescence measurements, the bandpass was 5 nm for both the excitation and emission slits in the experiments, except for studies involving the copper porphyrin when the slit was 20 nm on the excitation side. Equation 1 afforded corrections for the influence of absorbance

$$I_c = \frac{I}{1 - 10^{-A}} \quad (1)$$

where I is the experimental emission intensity, I_c is the corrected emission intensity, and A is the absorbance at the excitation wavelength.

For viscometry studies, solutions contained ST DNA at a concentration of 70 μM in base pairs. The mean length of the DNA molecules was ~3000 bp as established by gel electrophoresis by the supplier (GE Healthcare). Equation 2 gave the calculated standard reduced viscosity (SRV) ratio:

$$\frac{\eta}{\eta_0} = \frac{t_c - t_0}{t_D - t_0} \quad (2)$$

where t_0 is the flow time of the buffer, t_D is the flow time of DNA in buffer, and t_c is the flow time of the DNA solution containing porphyrin (*38*). For each measurement at 28.0 °C, the experimental flow time was the average of the first three consecutive runs that agreed with each other to within ±1 s. The buffer was a $\mu = 0.05$ M, pH 7.50 Tris solution, and immersion in a standard water bath provided a constant-temperature environment. The Purdue University Campus-Wide Mass Spectrometry Center took all mass spectrometry measurements, and D. Lee performed all microanalyses.

Linear dichroism experiments involved measuring the difference in the absorption of light polarized parallel and perpendicular to the flow direction as expressed in eq 3:

$$LD = A_{||} - A_{\perp} = A \times LD^r \quad (3)$$

where LD denotes the linear dichroism at wavelength λ (*39*, *40*). Equation 3 also defines the reduced linear dichroism signal (LD^r) which is the LD response divided by the isotropic absorbance A, at each wavelength.

Instrumentation

A Varian Cary 100 Bio UV−visible spectrophotometer, a Jasco V-550, or a Varian Cary 100 Scan UV−visible spectrophotometer provided absorbance data. The fluorescence spectrophotometer was a Varian Cary Elipse model,

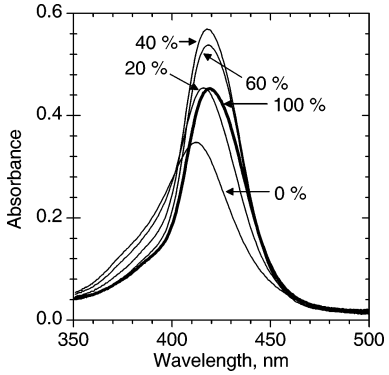

FIGURE 1: Absorption spectrum of a 4.0×10^{-6} M solution of Cu(tMe_2D4) as a function of volume percent of MeOH in 0.05 M Tris buffer (pH 7.5). The thick trace is 100% MeOH.

complete with an R3896 phototube, and the circular dichroism (CD) spectropolarimeter was a JASCO model J810. The NMR spectrometer was an Inova 300 MHz unit. A modified Cannon-Fenske model 25 viscometer was used. Other routine equipment used included a Corning model 430 pH meter and a Kenmore microwave oven. The LD instrument was a modified Jasco J-715 spectropolarimeter used in conjunction with a quartz Couette flow cell. One experiment involved the use of a microvolume Couette flow cell (*41*).

RESULTS

Porphyrin Synthesis. Combining 5-Me-DPM with 4-pyridinecarboxaldehyde to produce H_2tMe_2D4n is a variation of the 2+2 method for porphyrin synthesis (*30*, *42*, *43*) and is analogous to the route used previously for the synthesis of H_2D4n (*18*). The motivation behind the introduction of methyl substituents into positions 5 and 15 drew in part from a paper by Longo and co-workers (*44*), who proposed that tetrasubstituted derivatives like H_2tMe_2D4n naturally form in higher yield than a less substituted porphyrin such as H_2-D4. The argument is that, as condensation occurs, substituent groups induce coiling of the oligomer and thereby enhance the probability of ring closure. Although a subsequent paper cast doubt on the proposed substituent effect (*45*), the isolated yield of H_2tMe_2D4n is ~4% and consistently greater than (ca. 4 times) the yield obtained for H_2D4n. Methylation of H_2tMe_2D4n with methyl-*p*-toluenesulfonate gives the dication H_2tMe_2D4 which exhibits a Soret absorption maximum at 416 nm in aqueous solution. The overall yield is modest but practicable for the synthesis and characterization of new metalated forms. As an aside, it is worth noting that Gonçalves et al. reported a higher-yield synthesis of H_2D4 after the current study was complete (*46*).

Heating a DMF solution containing H_2tMe_2D4 and excess zinc(II) or copper(II) acetate leads to insertion of zinc(II) or copper(II) into the porphyrin (*47*). Treating the free porphyrin with aqueous acid (*48*) before inserting copper minimizes the chances of contamination with the much stronger lumaphor Zn(tMe_2D4). The zinc derivative Zn(tMe_2D4) has its Soret maximum at 428 nm. The Soret band of the Cu(tMe_2D4) system is different in that it is comparatively broad and has a low apparent molar absorptivity in aqueous solution. The molar absorptivity of Cu(tMe_2D4) also increases in methanol (Figure 1), whereas the absorbance of H_2tMe_2D4 or Zn(tMe_2D4) decreases by ~3%. As Figure 1 shows, the absorption intensity of Cu(tMe_2D4) is actually

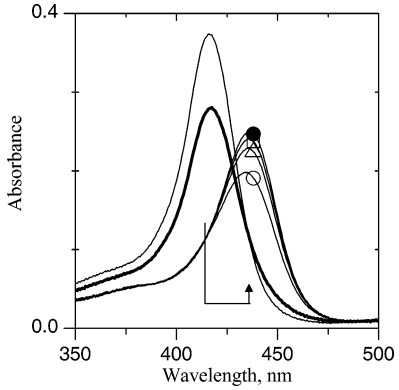

FIGURE 2: Absorbance of H_2tMe_2D4 in 0.05 M Tris buffer (pH 7.5) containing ST DNA at base pair-to-porphyrin ratios of 0 (thin trace), 1 (thick trace), 10 (○), 25 (△), 50 (□), and 100 (●).

highest in a solution that is ~40% methanol by volume. The absorbance increase at low methanol percentages is attributable to the dissociation of aggregated forms of Cu(tMe_2D4); see below for more evidence of aggregation phenomena. At higher methanol percentages, the absorbance decreases because the absorptivity of the monomer is inherently smaller in alcohol. In the absence of DNA, a 50% methanol/Tris buffer solution is a convenient solvent for absorbance comparisons with DNA-containing samples because Cu(tMe_2D4) exists as a monomer. The Soret maximum then occurs at 419 nm.

DNA Binding of H_2tMe_2D4. The data in Figure 2 reveal that the addition of ST DNA gives rise to three distinct modes of interaction with H_2tMe_2D4. The first occurs when the porphyrin is in excess and the base pairs-to-porphyrin quotient (q) is less than or equal to 1. Under these conditions, interaction with the host produces a hypochromic response in the Soret region but little or no spectral shift. There is also effectively no induced CD signal in the Soret region. The second type of adduct develops under conditions of intermediate loading ($2 \leq q \leq 10$), as evidenced both by a shift of the Soret band to a longer wavelength and the enhanced hypochromic response. Finally, the third mode of binding becomes evident when $q \geq 10$, when excess DNA is present in solution. In this regime, the wavelength of the Soret maximum shifts to a slightly longer wavelength, while the absorption intensity trends upward and asymptotically approaches a limiting hypochromicity (H) value of 32%. At the same time, the negative induced CD signal achieves a limiting amplitude ($\Delta\epsilon$) of -17 M^{-1} cm^{-1} at 440 nm (Table 1). Farther into the UV region, the induced CD spectrum includes a positive band at 370 nm. Binding also affects the emission of the porphyrin. The corrected emission spectrum of the free porphyrin is broad and weakly structured with a 0−0 band at 670 nm and a shoulder, with an intensity approximately half as great, at ~720 nm. In the presence of excess ST DNA, the emission intensity approximately doubles, and the resolution improves. The 0−0 band of the adduct occurs at 681 nm, while the adjoining 1−0 band appears at 746 nm and seems to weaken in intensity.

A similar sequence of events occurs with [poly(dG-dC)]$_2$ or [poly(dA-dT)]$_2$ as the host. The spectral changes are larger with the [poly(dG-dC)]$_2$ host, and by the time $q = 10$, the bathochromic shift of the Soret band is greater than 20 nm. With the addition of more [poly(dG-dC)]$_2$, the absorption maximum shifts further toward the red, while the absorption

Table 1: Spectral Data Obtained in 0.05 M Tris Buffer (pH 7.5)[a]

	$\Delta\lambda$ (nm) (%H)[b]	λ_{CD} (nm) [$\Delta\epsilon$ (M^{-1} cm^{-1})]	λ_{em} (nm)[c]
H_2tMe_2D4			670, 720sh
[poly(dA-dT)]$_2$	18 (14)	438 (−13)	679, 744
[poly(dG-dC)]$_2$	27 (40)	444 (−20)	690, 757
ST DNA	21 (32)	440 (−17)	681, 746
Cu(tMe_2D4)			
[poly(dA-dT)]$_2$	16 (32)	434 (−18)	821 broad
[poly(dG-dC)]$_2$	23 (52)	442 (−20)	822 broad
ST DNA	18 (50)	434 (−17)	820 broad
Zn(tMe_2D4)			670, 710sh
[poly(dA-dT)]$_2$	5 (15)	425 (+31) 449 (−25)	650, 705sh
[poly(dG-dC)]$_2$	18 (48)	~426 (+4) 454 (−5)	675, 719sh
ST DNA	9 (32)	424 (+6) 450 (−12)	657, 713sh

[a] When DNA is present, the data are for the limiting adducts formed at high base pair-to-porphyrin ratios. [b] Hypochromism (%H) is the percent change in absorbance at the absorption maximum. [c] From corrected spectra, except for the Cu(tMe_2D4) system which emits at longer wavelengths where the instrumental correction factors are less reliable.

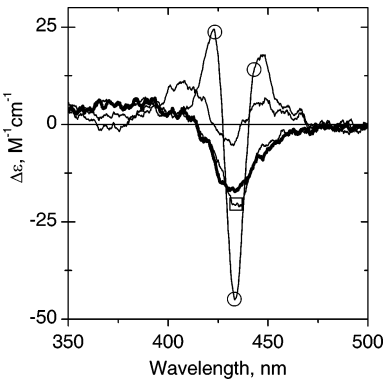

FIGURE 3: Induced CD spectra of Cu(tMe_2D4) in 0.05 M Tris buffer (pH 7.5) containing [poly(dA-dT)]$_2$ at q values of 1 (thin trace), 3 (○), 25 (□), and 100 (thick trace).

intensity increases and levels off when $H = 40\%$ by $q = 75$. Here, too, the limiting adduct shows two induced CD bands in the near UV, a negative band at 444 nm ($\Delta\epsilon = -20$ M^{-1} cm^{-1}) and a positive band at 370 nm ($\Delta\epsilon = 12$ M^{-1} cm^{-1}). Formation of an adduct with [poly(dA-dT)]$_2$ follows a similar pattern. At $q = 10$, the induced CD signal is multisignate, but the structure disappears when higher levels of [poly(dA-dT)]$_2$ are present. The limiting induced CD spectrum parallels that obtained with ST DNA or [poly(dG-dC)]$_2$ in exhibiting a negative band in the Soret region at 438 nm ($\Delta\epsilon = -13$ M^{-1} cm^{-1}) as well as a second band at a higher energy.

DNA Binding of Cu(tMe_2D4). Like H_2tMe_2D4, Cu(tMe_2-D4) experiences three distinct binding environments during a DNA titration. At low levels of [poly(dA-dT)]$_2$, when $q < 2$, the induced CD signal is weak and trisignate, but it becomes much more intense during the intermediate phase of binding [$2 \leq q \leq 10$ (Figure 3)]. In the final phase of binding, by $q = 25$, the signal devolves into a negative band with the extreme at ~434 nm. In contrast, the emission signal exhibits a relatively simple progression. Prior to the addition of [poly(dA-dT)]$_2$, there is no detectable emission from Cu(tMe_2D4), as one would expect because of solvent-induced quenching (*4*, *49*, *50*). However, the signal begins to grow with the addition of [poly(dA-dT)]$_2$; see Figure 4. By $q =$

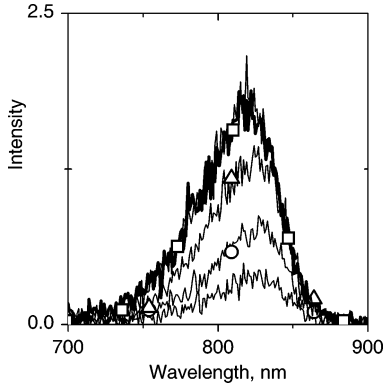

FIGURE 4: Absorbance-corrected emission spectra of Cu(tMe_2D4) in the presence of $[poly(dA\text{-}dT)]_2$ and 0.05 M Tris buffer (pH 7.5) at q values of 0.5 (thin trace), 1 (○), 2 (△), 10 (□), and 75 (thick trace). The $q = 10$ and 75 spectra virtually coincide.

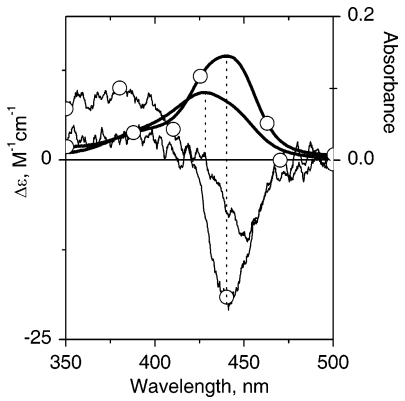

FIGURE 5: Induced CD spectra (thin traces) and absorbance spectra (thick traces) of Cu(tMe_2D4) in 0.05 M Tris buffer (pH 7.5) containing $[poly(dG\text{-}dC)]_2$ at q values of 2 (thick trace) and 75 (○). A dashed line relates corresponding spectra at the wavelength of the absorption maximum.

4, the signal essentially reaches a limiting emission intensity, albeit orders of magnitude weaker than the signal from H_2-tMe_2D4. The results differ only in detail when $[poly(dG\text{-}dC)]_2$ acts as the host. Most importantly, there is never an indication of a trisignate-induced CD signal. Instead, under conditions of intermediate loading ($2 \leq q \leq 10$), interaction with $[poly(dG\text{-}dC)]_2$ induces a bisignate but largely negative CD signal in the Soret region. The bisignate character is evident from the fact that the minimum occurs at around 450 nm, whereas the absorption is maximized at a significantly shorter wavelength (Figure 5). However, upon addition of excess DNA, the CD signal intensifies and shifts toward a higher energy until the band positions agree in the CD and absorption spectra. With this host, the emission signal from Cu(tMe_2D4) is maximized by $q \simeq 2$ and is ~3 times as intense as that obtained with $[poly(dA\text{-}dT)]_2$.

Qualitatively similar results are obtained with sonicated ST DNA as the host. Thus, the largest hypochromic response ($H \approx 67\%$) occurs in the absorption spectrum of Cu(tMe_2D4) under high loading conditions ($q \leq 3$), when there is almost no shift in the wavelength of the Soret maximum. Even though the emission signal from Cu(tMe_2D4) stops changing by $q = 3$, the largest shift of the Soret absorption occurs in the intermediate-loading regime ($3 \leq q \leq 10$). In the intermediate-loading regime, the system also maintains an isosbestic point at 410 nm; however, a new isosbestic point develops at 419 nm when the base pair-to-copper ratio

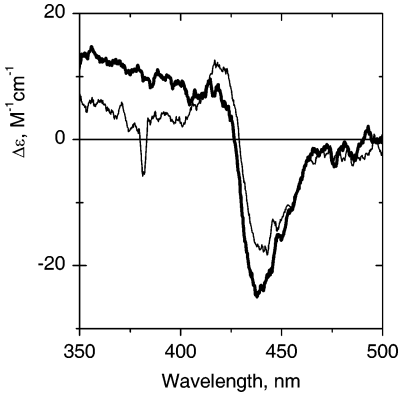

FIGURE 6: Induced CD spectrum of Cu(tMe_2D4) in 0.05 M Tris buffer (pH 7.5) containing ST DNA at a q value of 14 at ionic strengths of 0.05 M (thick trace) and 0.45 M (thin trace).

increases beyond 25. During formation of the final adduct, the hypochromism approaches a limiting value of ca. 50%. The CD results track those obtained with $[poly(dG\text{-}dC)]_2$ as the host.

Effect of Ionic Strength. Increasing the ionic strength has a modest effect on the spectral properties of Cu(tMe_2D4) interacting with ST DNA. As the ionic strength ranges from 0.05 to 0.45 M at $q = 14$, the Soret maximum shifts from 431 to 427 nm and the absorbance drops by 22%. Figure 6 portrays CD data obtained at either end of the ionic strength range. Bisignate character is apparent at $\mu = 0.45$ M where the spectrum shows a negative band at 442 nm as well as a weaker positive peak that is maximal around 420 nm. However, there is no shift of either the emission maximum or the emission intensity, after correcting for the absorbance change.

DNA Binding of Zn(tMe_2D4). Zn(tMe_2D4) is different in that it apparently exhibits only two phases of binding. When the porphyrin binds to $[poly(dG\text{-}dC)]_2$, there is no significant change in the emission spectrum, but there are changes in the electronic absorption. Thus, by $q \approx 10$, the Soret band experiences a bathochromic shift, and the hypochromic response sets in at even lower ratios. Compared with that of Cu(tMe_2D4), relatively high levels of $[poly(dG\text{-}dC)]_2$ are necessary to force formation of the limiting spectrum ($q \geq 100$). Nevertheless, binding induces sizable shifts in the absorbance maximum and intensity (Table 1). At saturation, the induced CD spectrum exhibits a minimum at ca. 454 nm and crosses zero at around 443 nm, essentially at the wavelength of the absorption maximum. Thus, the absorbance and CD data obtained for the final adduct mimic those of the adduct that Cu(tMe_2D4) forms with the same $[poly(dG\text{-}dC)]_2$ host during the intermediate phase of binding. Zn(tMe_2D4) also experiences only two binding environments in a titration with $[poly(dA\text{-}dT)]_2$. However, the absorption spectrum exhibits a relatively small bathochromic shift and practically no hypochromism when the porphyrin binds to $[poly(dA\text{-}dT)]_2$. Binding to $[poly(dA\text{-}dT)]_2$ is also distinctive in that the emission signal shifts toward a shorter wavelength. Furthermore, all spectral changes are complete by $q \approx 50$. See Figure 7 for representative CD spectra. At saturation, the signal exhibits a positive shoulder at ~400 nm beside a moderately intense bisignate signal that crosses over the baseline at 437 nm, ~5 nm beyond the absorption maximum.

Combined Uptake. Simultaneously exposing DNA to Cu(tMe_2D4) and Zn(tMe_2D4) provides a means of exploring

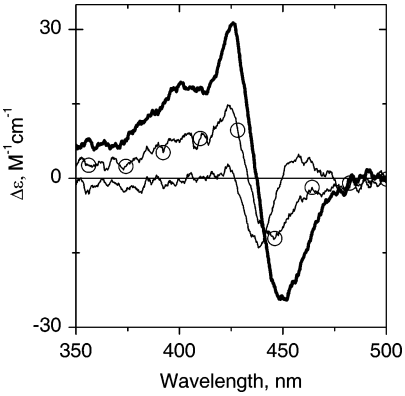

FIGURE 7: Induced CD spectra of Zn(tMe$_2$D4) in 0.05 M Tris buffer (pH 7.5) containing [poly(dA-dT)]$_2$ at q values of 1 (thin trace), 7 (○), and 50 (thick trace).

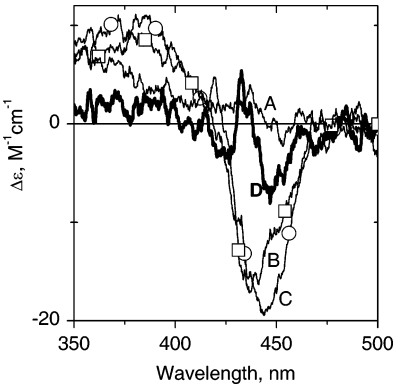

FIGURE 8: Induced CD spectra of porphyrins in 0.05 M Tris buffer (pH 7.5) with [poly(dG-dC)]$_2$ as the host. Samples contained Zn(tMe$_2$D4) at $q = 10$ (A, thin trace), Cu(tMe$_2$D4) at $q = 10$ (B, □), or Zn(tMe$_2$D4) and Cu(tMe$_2$D4), in which case the base pair-to-porphyrin ratio is 10 for each porphyrin (C, ○). The calculated difference spectrum (D, thick trace) represents spectrum C minus spectrum B.

cooperative effects. No unusual effects are evident when [poly(dA-dT)]$_2$ acts as the host, but the shift in the fluorescence maximum suggests that the uptake of Zn(tMe$_2$D4) is virtually complete when the base pairs-to-porphyrin ratio is 10 for each porphyrin. There is definitely a specific interaction with Zn(tMe$_2$D4) because the DNA absorption at 260 nm appears in the fluorescence excitation spectrum of the porphyrin. Cooperative binding is easier to recognize when Zn(tMe$_2$D4) interacts with [poly(dG-dC)]$_2$, because the affinity is comparatively low. Here, CD data clearly reveal that uptake of the copper porphyrin promotes binding of Zn(tMe$_2$D4). Results in Figure 8 show, for example, that Zn(tMe$_2$D4) contributes to the CD signal when [poly(dG-dC)]$_2$ is the host and each porphyrin is present at a DNA base pair-to-porphyrin ratio of 10. However, there is no significant signal from Zn(tMe$_2$D4) at the same loading level in the absence of Cu(tMe$_2$D4).

Viscometry. Viscometry measurements are useful because intercalation of a ligand into the DNA macromolecule has a measurable effect on the flow properties (*51*, *52*). In this study, the solutions contain a fixed concentration of sonicated ST DNA, while the porphyrin-to-base pair ratio, R, varies. The results in Figure 9 show that the specific viscosity increases by a factor of ~2 with the addition of H$_2$tMe$_2$D4, or Cu(tMe$_2$D4), before leveling of at ca. $R = 0.8$. At higher loadings ($R = 1.0$), the viscosity drops sharply in the case

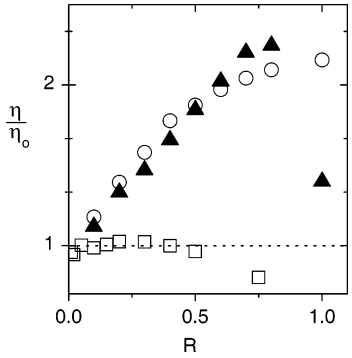

FIGURE 9: Standard reduced viscosity ratios as a function of the porphyrin-to-DNA base pair ratio R. The medium is 0.05 M Tris buffer (pH 7.5), and H$_2$tMe$_2$D4 (○), Cu(tMe$_2$D4) (▲), and Zn(tMe$_2$D4) (□) were employed as ligands.

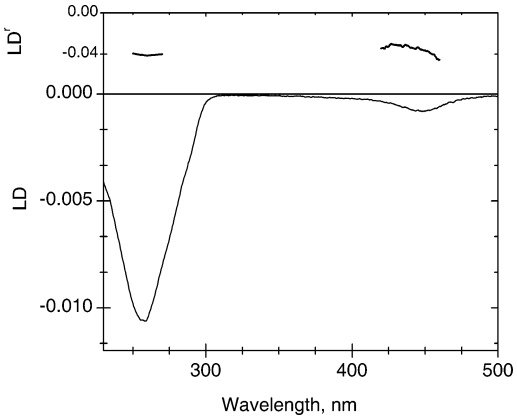

FIGURE 10: Linear dichroism of Zn(tMe$_2$D4) interacting with [poly(dG-dC)]$_2$ in 0.05 M Tris buffer (pH 7.8): (bottom) LD spectrum at a base pair-to-porphyrin ratio of 60 and (top) LD^r data for the same sample.

of Cu(tMe$_2$D4), presumably because the porphyrin aggregates on the surface of the DNA. On the other hand, uptake of Zn(tMe$_2$D4) produces quite different results. Thus, there is only a hint of an increase in the specific viscosity at low R values, before a noticeable decrease begins to occur at $R >$ 0.4.

Linear Dichroism. Figure 10 shows LD and LD^r spectra of Zn(tMe$_2$D4) interacting with [poly(dG-dC)]$_2$ at $q = 60$. Results obtained with Zn(T4) and H$_2$T4 are very similar. Due to the flow-induced ordering of the polymer, slightly more DNA molecules on average have a parallel orientation in solution. As the $\pi-\pi^*$ transitions of the bases are in-plane polarized and the base pairs are all more or less perpendicular to the long axis of B-form DNA, the LD and LD^r signals in Figure 10 are negative in the vicinity of 260 nm, in line with eq 3 ($A_\perp > A_{||}$). The corresponding LD^r signal at 440 nm is due only to the porphyrin and is almost equally negative. It follows that the porphyin ligand is roughly perpendicular to the long axis of DNA, too, because the Soret band is also $\pi-\pi^*$ absorption of a planar, aromatic ring system. Note that the LD^r signal in Figure 10 actually underestimates the dichroic response in the Soret region because there is still free Zn(tMe$_2$D4) in solution at $q = 60$. (Other data obtained with a microvolume Couette cell revealed that the magnitude of the LD response in the Soret region signal increased by ca. 40% relative to that observed in the 260 nm region at $q = 75$. However, the latter experiment required a higher porphyrin concentration, and

a precipitate formed before it was possible to gather the absorbance data needed for calculation of an accurate LD^r spectrum.) The conclusion is that the LD data obtained at $\mu = 0.05$ M for Zn(tMe_2D4), Zn(T4), and H_2T4 are all consistent with intercalative binding to [poly(dG-dC)]$_2$.

DISCUSSION

The following questions remain: What modes of binding unfold as DNA takes up H_2tMe_2D4 or Cu(tMe_2D4)? Why is the uptake of Zn(tMe_2D4) a qualitatively different process? Do the steric demands of the methyl substituents at positions 5 and 15 of H_2tMe_2D4 impact the binding to DNA? And, is there any evidence of cooperative uptake? As a prelude to the resolution of these issues, a brief summary of some important background is useful.

Aggregation Effects

Aggregation is an important effect to consider in aqueous media because porphyrins have such a hydrophobic core, although the charged periphery provides a countervailing force. Sterically active substituents may also affect the process as indicated by the work of Tjahjono and co-workers (*53*), who found that the dication 5,15-bis(1,3-dimethylimidazolium-2-yl)porphyrin exists as a monomer in water whereas the more planar 5,15-bis(1,2-dimethylpyrazolium-4-yl)porphyrin undergoes extensive aggregation. In the case of the tetracationic porphyrin H_2T4, the repulsive effects completely dominate, because H_2T4 exists as a monomer under normal conditions (*54*, *55*). However, the dicationic analogue H_2T_{agg} behaves differently. It shows a strong tendency to aggregate as evidenced by a broadened Soret band, diminished absorbance intensity, and increased dynamic light scattering (*29*). Furthermore, codissolved DNA macromolecules enhance the effect by serving as templates for aggregation (*24*, *56*). Since H_2tMe_2D4 and its various derivatives are dicationic porphyrins, aggregation is something to consider.

Luminescence and Copper(II) Porphyrins

Luminescence studies of copper(II) porphyrins provide unique insight into DNA binding interactions. One reason is that the emission signal is extremely sensitive to the local environment about the copper center. Another plus, which will be important in the discussion below, is that through-space coupling with other chromophores does not affect the signal. The steric demands of the copper(II) form are also similar to those of the free porphyrin. Thus, in the electronic ground state, copper(II) porphyrins tend not to bind axial ligands because the "hole" in the d^9 shell of the copper center resides in the plane of the porphyrin, i.e., in the $d_{x^2-y^2}$ orbital. Thermal population of a five-coordinate structure is normally not feasible except in the presence of a very strong base such as pyridine (*57*). However, it is important to recognize that axial ligands have a profound influence on the excited state dynamics. The luminescence spectra of a free porphyrin and its copper(II) derivative are always very different. While the free porphyrin exhibits fluorescence from a $^1\pi-\pi^*$ excited state, the four-coordinate copper(II) derivative emits from a lower-energy state (with a multiplet structure) derived from the corresponding triplet intraligand excited state (*58*). Multiplicity changes are rapid in the copper(II) derivative due to the presence of the unpaired electron on the central metal ion. In addition, efficient quenching by Lewis bases, including water, is unique to the copper(II) form. Formation of a five-coordinate adduct is feasible in the excited state because the hole can migrate to the d_{z^2} orbital (*16*, *49*, *50*, *59*−*62*). The five-coordinate form is nonemissive because radiationless decay is facile and because d−d states have intrinsically low dipole strengths. Observation of the five-coordinate d−d excited state has been possible with a time-resolved X-ray absorption technique (*63*), as well as by time-resolved resonance Raman spectroscopy (*64*). Indeed, Raman studies have shown that formation of a photoexcited, five-coordinate form is virtually obligatory whenever a copper(II) porphyrin binds externally to single- or double-stranded DNA (*50*, *65*, *66*). The only way the emission survives is if the DNA host shields the axial positions of the copper(II) center from attack by solvent, buffer, and/or Lewis bases embedded in the DNA host. Observation of emission from bound Cu(T4) therefore proves to be the signature of intercalative binding (*16*, *49*, *62*). Szalai and co-workers (*67*) have used a similar strategy to establish that Cu(T4) is also capable of internalizing into quadruplex-forming host structures.

Interactions of DNA with H_2tMe_2D4 and Cu(tMe_2D4)

With all three porphyrins and H_2tMe_2D4 and Cu(tMe_2D4) in particular, the nature of the adduct that forms and the consequent spectral changes depend very much on the DNA base pair-to-porphyrin ratio (q) in solution. The interpretation is most straightforward when DNA is present in large excess.

Excess DNA Regime ($q \geq 25$). When excess DNA is present, both H_2tMe_2D4 and Cu(tMe_2D4) bind as intercalators. Primary indicators are the hyperchromic responses and negative CD signals, both diagnostic of intercalative binding (*3*, *4*). Another sign of intercalation is the increase in the specific viscosity of ST DNA that occurs with the uptake of H_2tMe_2D4 or Cu(tMe_2D4) (*52*). The viscosity enhancement occurs because intercalation of a ligand results in an increase in the average length and rigidity of the DNA molecule. In turn, the length increase enhances the resistance to flow as long as the average chain length is compatible with rodlike diffusion (*68*). Last but not least, the adducts formed by Cu(tMe_2D4) and DNA are luminescent. Studies have shown that emission quenching is virtually complete when the analogous Cu(T4) complex binds externally to [poly(dA-dT)]$_2$ (*49*). Intercalation is the only mode of binding that completely blocks access to the axial coordination positions about the copper center. It is interesting in this regard that both the intensity and the wavelength maximum of the emission from the bound form of Cu(tMe_2D4) vary with the DNA host. In particular, the intensity is ~3 times higher for adduct formation with [poly(dG-dC)]$_2$ than with [poly(dA-dT)]$_2$. A similar emission increase occurs when Cu(T4) migrates to a DNA host with higher melting temperatures (*16*, *62*). A possible explanation is that, during the lifetime of the excited state, structural fluctuations of the host periodically expose the copper center to quenching centers. In that case, the emission intensity varies with the rigidity of the host. When an A=T base pair is part of the intercalation site, free thymine C=O groups are also available to act as nucleophiles.

Intermediate Loading ($2 \leq q \leq 20$). In the intermediate-loading regime when $2 \leq q \leq 20$, the picture is a bit more complicated, but intercalation is still the favored binding motif for H_2tMe_2D4 and Cu(tMe_2D4). The analysis focuses on the results with the copper derivative. To start, the hypochromism induced by the addition of ST DNA, [poly(dG-dC)]$_2$, or [poly(dA-dT)]$_2$ as well as the viscometry data obtained with ST DNA is consistent with intercalation of Cu(tMe_2D4). However, the emission results definitively establish that the binding is by intercalation. The onset of the emission signal coincides with the appearance of [poly(dG-dC)]$_2$ or [poly(dA-dT)]$_2$ in solution, and in both cases, the emission intensity saturates by around $q = 3$. Intercalated Cu(tMe_2D4) is undoubtedly the only contributing species, because neither the emission maximum nor the intensity changes with the addition of excess DNA. If a second emitting species were present, some change in the signal would occur because the emission from Cu(tMe_2D4) is very sensitive to the nature and rigidity of the host, vide supra.

With foreknowledge of the mode of binding, interpretation of the relatively complicated CD becomes feasible. For example, it is easy to understand why the adduct of Cu(tMe_2D4) with [poly(dA-dT)]$_2$ exhibits a multisignate CD spectrum at $q = 3$ (Figure 3), even though the porphyrin binds by intercalation. The problem is that excitonic coupling between neighboring transition moments is unavoidable at such a high loading (*69*). In the literature, there are many reports of bisignate, or bimodal, induced CD signals attributed to self-stacking of cationic porphyrins on the exterior of a polyanionic DNA host (*24*, *29*). However, exciton coupling depends upon proximity, not self-stacking. Elegant studies by Lewis and co-workers (*70*) have demonstrated that stilbene chromophores couple through as many as 10 bp in doubly capped hairpins. Nakanishi and co-workers (*71*) have reported similar effects in solutions containing porphyrin chromophores tethered to opposite ends of DNA duplexes. For a noncovalently bound chromophore, such as Cu(tMe_2D4), the spacing between chromophores may vary, but neighbor−neighbor interactions are inevitable at low q values (high loading) because of the limited pool of available binding sites.

Heavy Loading Regime. Finally, a very different mode of binding occurs at the highest loadings, when $q < 2$. In many respects, this regime is notable for the lack of spectroscopic consequences. Witness, for example, the lack of intensity in the induced CD spectrum and the absence of a significant bathochromic shift in the Soret region. The bound form of Cu(tMe_2D4) is practically nonemissive as well. Indeed, when the DNA base pair-to-porphyrin ratio is small, hypochromism is the major spectral perturbation, as is the case when porphyrins aggregate in aqueous solution (*29*). When there is too little DNA in solution to take up the ligand, it seems clear that the host simply serves to provide nucleation sites for aggregation of the porphyrin.

Interactions of DNA with Zn(tMe_2D4)

In contrast to Cu(tMe_2D4) and H_2tMe_2D4, Zn(tMe_2D4) apparently exhibits only two phases of binding. Moreover, as the discussion will show, near-neighbor porphyrin−porphyrin interactions persist even in the presence of a large excess of DNA due to cooperative uptake of Zn(tMe_2D4).

Zn(tMe_2D4) and [Poly(dG-dC)]$_2$. Titrating in small amounts of [poly(dG-dC)]$_2$ clearly promotes the aggregation of the Zn(tMe_2D4) porphyrin. Thus, the hypochromism in the Soret band reaches 40% by $q = 10$, despite almost no change in band position and the absence of a significant induced CD signal. By $q = 20$, however, the second, apparently final phase of binding starts to appear. In this loading regime, the hypochromism continues to increase marginally; the new effect is a bathochromic shift of the Soret absorption. When excess [poly(dG-dC)]$_2$ is present, the decrease in hypochromism is very slight, so it seems evident that Zn(tMe_2D4) binds as an intercalator. The LD^r results in Figure 10 support this interpretation. The intercalation of Zn(tMe_2D4) is not so surprising when one recognizes that same experiments reveal that Zn(T4) also intercalates into [poly(dG-dC)]$_2$. The latter observation should draw attention because previous LD studies have found that Zn(T4) binds externally to calf thymus DNA, in a canted orientation relative to the DNA bases (*72*, *73*). One difference is that A=T base pairs outnumber G≡C base pairs in calf thymus DNA, but there is another important qualification to bear in mind as well. Namely, this study used a $\mu = 0.05$ M buffer, and Chirvony et al. (*74*) have already shown that the interaction between Zn(T4) and [poly(dG-dC)]$_2$ is very sensitive to ionic strength. Their analysis of hypochromism and triplet quenching data shows that intercalation is an important binding motif for Zn(T4) at lower ionic strengths ($\mu \approx 0.03-0.05$ M) but that external binding to [poly(dG-dC)]$_2$ becomes dominant at higher ionic strengths.

Two compensating effects account for the fact that uptake by [poly(dG-dC)]$_2$ has little effect on the emission maximum. One is that the zinc porphyrin has to dissociate an axial ligand to bind as an intercalator. If that were the only consideration, the emission would shift to a higher energy (*75*). However, intercalating between bases naturally induces a bathochromic shift of the emission. As demonstrated in previous binding studies involving Zn(D4) (*18*), the net result is little or no shift in the emission maximum. A self-stacked version of four-coordinate, externally bound Zn(tMe_2D4) arguably could give rise to similar absorbance and emission spectra. However, results obtained with the Cu(tMe_2D4) system have established that intercalation is the preferred binding motif for a porphyrin with an in-plane metal center and no axial ligands.

Self-stacking on the [poly(dG-dC)]$_2$ host would also give rise to a CD signal much stronger than the one observed here (*24*). Asymmetric and mainly negative, the induced CD signal of the Zn(tMe_2D4) adduct is clearly bisignate because the CD signal crosses the baseline at essentially the wavelength of the absorption maximum. The CD signal is still compatible with intercalative binding, because the adduct formed by Cu(tMe_2D4) and [poly(dG-dC)]$_2$ exhibits virtually the same band shape, under conditions of intermediate loading. The chromophores have to bind only close enough to each other to experience excitonic coupling. What makes the Zn(tMe_2D4) system unusual is that proximate spacing persists even at very high q values due to a cooperative effect, vide infra.

Zn(tMe_2D4) and [Poly(dA-dT)]$_2$. The zinc porphyrin also exhibits only two phases of binding with [poly(dA-dT)]$_2$. Here, too, the first phase of binding clearly involves aggregation of the porphyrin because the introduction of low

levels of the DNA generates an absorbance decrease but no appreciable shift in the Soret maximum. The approach toward a limiting spectrum begins by $q \approx 10$ base pairs per porphyrin, but Zn(tMe_2D4) clearly remains bound externally to $[poly(dA\text{-}dT)]_2$. The most telling effect is that the absorption spectrum of the limiting adduct exhibits almost no hypochromism. A four-coordinate form would intercalate into $[poly(dA\text{-}dT)]_2$ just as Cu(tMe_2D4) does, so Zn(tMe_2-D4) must retain a fifth ligand. Nevertheless, some type of structural reorganization occurs, because the emission signal undergoes a distinct hypsochromic shift. The shift in the emission may be an indication of weaker axial ligation (*75*), perhaps because a donor group from the DNA displaces the original water ligand. Kruglik et al. have invoked analogous adduct formation with $[poly(dA\text{-}dT)]_2$ to explain Raman results obtained for a photoexcited state of Cu(T4) (*76*). At this juncture, postulating coordinate−covalent bond formation to a DNA base is highly speculative, but that could also explain why irradiation at 260 nm into a short-lived state of $[poly(dA\text{-}dT)]_2$ produces emission from Zn(tMe_2D4). Previous workers have argued that DNA absorption becomes involved only in the porphyrin excitation spectrum when there is intercalative binding (*77*). In principle, covalent bonding to a DNA base could also give rise to a splitting of the Soret transition and account for the bisignate CD signal (*78*). However, the symmetry of the observed CD spectrum and the fact that the crossover wavelength agrees with the wavelength maximum of the Soret absorption are much more in keeping with a conservative spectrum. As with $[poly(dG\text{-}dC)]_2$, the Zn(tMe_2D4) ligands must bind close enough to each other on the $[poly(dA\text{-}dT)]_2$ host to experience exciton coupling (*78*).

Cooperative Effects. Evidence that points to cooperative binding of Zn(tMe_2D4) includes the difference spectrum in Figure 8 as well as with the bisignate CD spectra exhibited by the adducts formed with $[poly(dG\text{-}dC)]_2$ and $[poly(dA\text{-}dT)]_2$. In the context of cationic porphyrins, the most commonly recognized form of cooperative binding to DNA is self-stacking on the surface of the host (*25*, *29*, *79*). However, more traditional modes of ligand binding can also exhibit cooperativity when binding involves reorganization of the DNA structure (*80*). Whenever extending the reorganization to a neighboring position is easier than initiating a structure change somewhere else in the host, cooperative uptake is a possibility. Relative to Cu(tMe_2D4), the reorganization necessary for intercalation of the zinc(II) porphyrin entails an added energy requirement, namely, dissociation of an axial ligand (*18*, *21*). The affinity for Zn(tMe_2D4) is therefore weaker, and that may explain why cooperative effects become important. Creation of a cavity requires local unwinding of the host (*81*), and simply extending the structural change to a neighboring site may well facilitate the uptake of another Zn(tMe_2D4) ligand. Coulombic repulsion between ligands serves as a countervailing force, but the +2 charge of the ligand should not present much of a problem in the field of the DNA phosphates. Although not much structural information is available, a similar analysis can probably be applied to formation of adducts with $[poly(dA\text{-}dT)]_2$ because high-affinity external binding appears to involve substantial structural reorganization (*18*, *19*, *21*). As others have suggested (*82*, *83*), electrostatic effects and/or local hydration may well predispose a sequence that is rich in A=T base pairs to bind bulky porphyrins externally. It is, however, also true that porphyrins are rigid molecules that do not have the crescent shape normally found in ligands tailored for high-affinity groove binding to the canonical DNA structure. Structural reorganization of a flexible host therefore provides an opportunity to maximize interactions with the DNA surface.

CONCLUSIONS AND PERSPECTIVE

Tetrasubstituted H_2tMe_2D4 behaves more like the disubstituted porphyrin H_2D4 than H_2T4, because H_2tMe_2D4 and Cu(tMe_2D4) both intercalate into B-form DNA irrespective of its base composition. However, the steric consequences associated with the 5,15-methyl substituents become apparent with the weaker ligand Zn(tMe_2D4), which adopts an external binding motif in low-melting, A=T base pair-rich runs of DNA. Compared with H_2T4, the dicationic H_2tMe_2D4 system is more prone to aggregate on the DNA host; however, the problem is minimal by comparison with a really hydrophobic porphyrin like H_2T_{agg} (*29*). In order of increasing base pair-to-porphyrin ratios, the three environments that H_2tMe_2D4 or Cu(tMe_2D4) experiences in a typical DNA titration are surface aggregation, followed by densely spaced intercalation, and then dispersion into independent, well-separated intercalation sites. Uptake of Zn(tMe_2D4) is very different because binding is a strictly cooperative process and the motif depends on the base content of the DNA host. Heretofore, external stacking has been widely recognized as a binding motif compatible with cooperative uptake of a cationic porphyrin (*22*, *56*, *79*), but cooperative binding may occur whenever substantial structural reorganization is necessary. Recognizing when cooperative binding occurs is important because it impacts everything from competitive binding assays (*84*) to comparative kinetics studies (*85*, *86*).

In the case of porphyrins, through-space or through-bond interactions involving near neighbors complicate spectral analyses when the chromophores do not resonate independently. For example, one cannot assume that an intercalated porphyrin will give a negative induced CD signal in the Soret region, when other chromophores bind nearby. The reason is that coupling between chromophores produces a multisignate response that depends on the distance(s) of separation and therefore the loading. While dipole−dipole coupling is an excited state interaction, alteration of the spectral properties can complicate the process of extracting ground state information, such as the binding constant. Fortunately, dipole−dipole interactions do not affect the luminescence studies of copper(II) porphyrins due to the forbidden character of the transition. In DNA binding studies with Cu(tMe_2D4), data from emission and CD studies yield unusually detailed information about the intermediate loading regime. The emission results are notable because they establish that Cu(tMe_2D4) binds by intercalation and that the porphyrin has a footprint of ~3 bp. Juxtapositional metal-centered and $\pi-\pi^*$ excited states render the emission of a copper(II) porphyrin uniquely sensitive to the presence of Lewis bases (*4*, *21*, *49*, *62*). To cite examples, Lewis bases do not quench the emission of a palladium(II) porphyrin because the metal-centered states are inaccessible, while nickel(II) porphyrins are nonemissive because metal-centered excited states occur at relatively low energies (*87*, *88*).

REFERENCES

1. Fiel, R. J. (1989) Porphyrin-Nucleic Acid Interactions: A Review, *J. Biomol. Struct. Dyn. 6* (6), 1259−1275.
2. Marzilli, L. G. (1990) Medical Aspects of DNA-Porphyrin Interactions, *New J. Chem. 14* (6−7), 409−420.
3. Pasternack, R. F., and Gibbs, E. J. (1996) Porphyrin and metalloporphyrin interactions with nucleic acids, *Met. Ions Biol. Syst. 33*, 367−397.
4. McMillin, D. R., and McNett, K. M. (1998) Photoprocesses of copper complexes that bind to DNA, *Chem. Rev. 98* (3), 1201−1219.
5. Kessel, D., Luguya, R., and Vicente, M. G. H. (2003) Localization and photodynamic efficacy of two cationic porphyrins varying in charge distribution, *Photochem. Photobiol. 78* (5), 431−435.
6. Lang, K., Mosinger, J., and Wagnerova, D. M. (2004) Photophysical properties of porphyrinoid sensitizers non-covalently bound to host molecules: Models for photodynamic therapy, *Coord. Chem. Rev. 248* (3−4), 321−350.
7. Griffiths, J. (2004) Colourful Therapy, *Educ. Chem. 41* (3), 71−73.
8. Han, F. X. G., Wheelhouse, R. T., and Hurley, L. H. (1999) Interactions of TMPyP4 and TMPyP2 with quadruplex DNA. Structural basis for the differential effects on telomerase inhibition, *J. Am. Chem. Soc. 121* (15), 3561−3570.
9. Cech, T. R. (2000) Life at the end of the chromosome: Telomeres and telomerase, *Angew. Chem., Int. Ed. 39* (1), 35−43.
10. Carvlin, M. J., Dattagupta, N., and Fiel, R. J. (1982) Circular-Dichroism Spectroscopy of a Cationic Porphyrin Bound to DNA, *Biochem. Biophys. Res. Commun. 108* (1), 66−73.
11. Fiel, R. J., Howard, J. C., Mark, E. H., and Dattagupta, N. (1979) Interaction of DNA with a Porphyrin Ligand: Evidence for Intercalation, *Nucleic Acids Res. 6* (9), 3093−3118.
12. Carvlin, M. J., and Fiel, R. J. (1983) Intercalative and Nonintercalative Binding of Large Cationic Porphyrin Ligands to Calf Thymus DNA, *Nucleic Acids Res. 11* (17), 6121−6139.
13. Fiel, R. J., and Munson, B. R. (1980) Binding of Meso-Tetra(4-N-Methylpyridyl) Porphine to DNA, *Nucleic Acids Res. 8* (12), 2835−2842.
14. Pasternack, R. F., Gibbs, E. J., and Villafranca, J. J. (1983) Interactions of Porphyrins with Nucleic-Acids, *Biochemistry 22* (23), 5409−5417.
15. Strickland, J. A., Marzilli, L. G., and Wilson, W. D. (1990) Binding of Meso-Tetrakis(N-Methylpyridiniumyl)Porphyrin Isomers to DNA: Quantitative Comparison of the Influence of Charge-Distribution and Copper(II) Derivatization, *Biopolymers 29* (8−9), 1307−1323.
16. Eggleston, M. K., Crites, D. K., and McMillin, D. R. (1998) Studies of the base-dependent binding of Cu(T4) to DNA hairpins (H_2T4 = meso-tetrakis(4-(N-methylpyridiumyl))porphyrin), *J. Phys. Chem. A 102* (28), 5506−5511.
17. Gibbs, E. J., Maurer, M. C., Zhang, J. H., Reiff, W. M., Hill, D. T., Malickablaszkiewicz, M., McKinnie, R. E., Liu, H. Q., and Pasternack, R. F. (1988) Interactions of Porphyrins with Purified DNA and More Highly Organized Structures, *J. Inorg. Biochem. 32* (1), 39−65.
18. Bejune, S. A., Shelton, A. H., and McMillin, D. R. (2003) New Dicationic Porphyrin Ligands Suited for Intercalation into B-Form DNA, *Inorg. Chem. 42*, 8465−8475.
19. Tears, D. K. C., and McMillin, D. R. (1998) Duplex hydrogen banding promotes intercalation of Cu(T4) in DNA hairpins (Cu(T4) = meso-tetrakis(4-(N-methylpyridyl))porphyrincopper(II)), *Chem. Commun. 22*, 2517−2518.
20. Strickland, J. A., Marzilli, L. G., Gay, K. M., and Wilson, W. D. (1988) Porphyrin and Metalloporphyrin Binding to DNA Polymers: Rate and Equilibrium Binding Studies, *Biochemistry 27* (24), 8870−8878.
21. McMillin, D. R., Shelton, A. H., Bejune, S. A., Fanwick, P. E., and Wall, R. K. (2005) Understanding binding interactions of cationic porphyrins with B-form DNA, *Coord. Chem. Rev. 249* (13−14), 1451−1459.
22. Gibbs, E. J., Tinoco, I., Maestre, M. F., Ellinas, P. A., and Pasternack, R. F. (1988) Self-Assembly of Porphyrins on Nucleic-Acid Templates, *Biochem. Biophys. Res. Commun. 157* (1), 350−358.
23. Sari, M. A., Battioni, J. P., Dupre, D., Mansuy, D., and Lepecq, J. B. (1990) Interaction of Cationic Porphyrins with DNA: Importance of the Number and Position of the Charges and Minimum Structural Requirements for Intercalation, *Biochemistry 29* (17), 4205−4215.
24. Pasternack, R. F., Ewen, S., Rao, A., Meyer, A. S., Freedman, M. A., Collings, P. J., Frey, S. L., Ranen, M. C., and de Paula, J. C. (2001) Interactions of copper(Il) porphyrins with DNA, *Inorg. Chim. Acta 317* (1−2), 59−71.
25. Pasternack, R. F., Gibbs, E. J., and Villafranca, J. J. (1983) Interactions of Porphyrins with Nucleic Acids, *Biochemistry 22* (10), 2406−2414.
26. Lipscomb, L. A., Zhou, F. X., Presnell, S. R., Woo, R. J., Peek, M. E., Plaskon, R. R., and Williams, L. D. (1996) Structure of a DNA-porphyrin complex, *Biochemistry 35* (9), 2818−2823.
27. Guliaev, A. B., and Leontis, N. B. (1999) Cationic 5,10,15,20-tetrakis(N-methylpyridinium-4-yl)porphyrin fully intercalates at 5′-CG-3′ steps of duplex DNA in solution, *Biochemistry 38* (47), 15425−15437.
28. Wall, R. K., Shelton, A. H., Bonaccorsi, L. C., Bejune, S. A., Dube, D., and McMillin, D. R. (2001) H_2D3: A cationic porphyrin designed to intercalate into B-form DNA (H_2D3 = trans-di(N-methylpyridium-3-yl)porphyrin), *J. Am. Chem. Soc. 123* (46), 11480−11481.
29. Pasternack, R. F., Bustamante, C., Collings, P. J., Giannetto, A., and Gibbs, E. J. (1993) Porphyrin Assemblies on DNA as Studied by a Resonance Light-Scattering Technique, *J. Am. Chem. Soc. 115* (13), 5393−5399.
30. Lin, V. S. Y., Iovine, P. M., DiMagno, S. G., and Therien, M. J. (2002) Dipyrryl and porphyrinic precursors to supramolecular conjugated (porphinato)metal arrays: Synthesis of dipyrrylmethane and (5,15-diphenylporphinato)zinc(II), *Inorg. Synth. 33*, 55−61.
31. Manka, J. S., and Lawrence, D. S. (1989) High-Yield Synthesis of 5,15-Diarylporphyrins, *Tetrahedron Lett. 30* (50), 6989−6992.
32. Wang, Q. M., and Bruce, D. W. (1995) One-Step Synthesis of Beta,Meso-Unsubstituted Dipyrromethane, *Synlett 12*, 1267−1268.
33. Batinic-Haberle, I., Spasojevic, I., Hambright, P., Benov, L., Crumbliss, A. L., and Fridovich, I. (1999) Relationship among redox potentials, proton dissociation constants of pyrrolic nitrogens, and in vivo and in vitro superoxide dismutating activities of manganese(III) and iron(III) water-soluble porphyrins, *Inorg. Chem. 38* (18), 4011−4022.
34. Sambrook, J., Fritsch, J., and Maniatis, T. (1989) *Molecular Cloning: A Laboratory Manual*, 2nd ed., Cold Springs Harbor Laboratory Press, Plainview, NY.
35. Inman, R. B., and Baldwin, R. L. (1962) Helix-Random Coil Transitions in Synthetic DNAs of Alternating Sequence, *J. Mol. Biol. 5*, 172−184.
36. Grant, R. C., Kodama, M., and Wells, R. D. (1972) Enzymatic and Physical Studies on $(dI\text{-}dC)_n\cdot(dI\text{-}dC)_n$ and $(dG\text{-}dC)_n\cdot(dG\text{-}dC)_n$, *Biochemistry 11* (5), 805−815.
37. Felsenfeld, G., and Hirschman, S. Z. (1965) A Neighbor-Interaction Analysis of the Hypochromism and Spectra of DNA, *J. Mol. Biol. 13*, 407−427.
38. Satyanarayana, S., Dabrowiak, J. C., and Chaires, J. B. (1992) Neither Δ-Tris(phenanthroline)ruthenium(II) nor Λ-Tris(phenanthroline)ruthenium(II) Binds to DNA by Classical Intercalation, *Biochemistry 31* (39), 9319−9324.
39. Rodger, A. (1993) Linear Dichroism, *Methods Enzymol. 226*, 232−258.
40. Rodger, A., and Norden, B. (1997) *Circular Dichroism and Linear Dichroism*, Oxford University Press, New York.
41. Marrington, R., Dafforn, T. R., Halsall, D. J., MacDonald, J. I., Hicks, M., and Rodger, A. (2005) Validation of new microvolume Couette flow linear dichroism cells, *Analyst 130*, 1608−1616.
42. Lindsey, J. S. (1999) Synthesis of meso-Substituted Porphyrins, in *The Porphyrin Handbook* (Kadish, K. M., Smith, K. M., and Guilard, R., Eds.) pp 45−118, Academic Press, New York.
43. Vicente, M. G. H., and Smith, K. M. (2000) Porphyrins and derivatives: Synthetic strategies and reactivity profiles, *Curr. Org. Chem. 4*, 139−174.
44. Longo, F. R., Thorne, E. J., Adler, A. D., and Dym, S. (1975) Notes on the Synthesis of Porphin, *J. Heterocycl. Chem. 12*, 1305−1309.
45. Kim, J. B., Adler, A. D., and Longo, F. R. (1978) Synthesis of Porphyrins from Monopyrroles, in *The Porphyrins* (Dolphin, D., Ed.) pp 85−100, Academic Press, New York.
46. Goncalves, D. P. N., Ladame, S., Balasubramanian, S., and Sanders, J. K. M. (2006) Synthesis and G-quadruplex binding studies of new 4-N-methylpyridinium porphyrins, *Org. Biomol. Chem. 4*, 3337−3342.

47. Asano-Someda, M., and Kaizu, Y. (1995) Red-Shifted Emission Spectra of Several Mesosubstituted Copper Porphyrins in Fluid Solution, *J. Photochem. Photobiol., A 87*, 23−29.
48. Shah, B., and Hambright, P. (1970) Acid Catalyzed Solvolysis Reactions of Zinc Porphyrins, *J. Inorg. Nucl. Chem. 32*, 3420−3422.
49. Hudson, B. P., Sou, J., Berger, D. J., and McMillin, D. R. (1992) Luminescence Studies of the Intercalation of Cu(TMPyP4) into DNA, *J. Am. Chem. Soc. 114*, 8997−9002.
50. Mojzes, P., Chinsky, L., and Turpin, P. Y. (1993) Interaction of Electronically Excited Copper(II) Porphyrin with Oligonucleotides and Polynucleotides: Exciplex Building Process by Photoinitiated Axial Ligation of Porphyrin to Thymine and Uracil Residues, *J. Phys. Chem. 97*, 4841−4847.
51. Saucier, J. M., Lepecq, J. B., and Festy, B. (1971) Change of Torsion of DNA Helix Caused by Intercalation. 2. Measurement of Relative Change of Torsion Induced by Various Intercalating Drugs, *Biochimie 53*, 973−980.
52. Banville, D. L., Marzilli, L. G., Strickland, J. A., and Wilson, W. D. (1986) Comparison of the Effects of Cationic Porphyrins on DNA Properties: Influence of GC Content of Native and Synthetic Polymers, *Biopolymers 25*, 1837−1858.
53. Tjahjono, D. H., Yamamoto, T., Ichimoto, S., Yoshioka, N., and Inoue, H. (2000) Synthesis and DNA-binding properties of bisdiazoliumylporphyrins, *J. Chem. Soc., Perkin Trans. 1*, 3077−3081.
54. Pasternack, R. F., Centuro, G. C., Boyd, P., Hinds, L. D., Huber, P. R., Francesc, L., Fasella, P., Engasser, G., and Gibbs, E. (1972) Aggregation of Meso-Substituted Water-Soluble Porphyrins, *J. Am. Chem. Soc. 94*, 4511−4517.
55. Kano, K., Fukuda, K., Wakami, H., Nishiyabu, R., and Pasternack, R. F. (2000) Factors influencing self-aggregation tendencies of cationic porphyrins in aqueous solution, *J. Am. Chem. Soc. 122*, 7494−7502.
56. Pasternack, R. F., Giannetto, A., Pagano, P., and Gibbs, E. J. (1991) Self-Assembly of Porphyrins on Nucleic Acids and Polypeptides, *J. Am. Chem. Soc. 113*, 7799−7800.
57. Szintay, G., Horvath, A., and Grampp, G. (1999) Temperature dependence study of pyridine complex formation and emission quenching of copper(II) octaethyl- and tetraphenylporphyrin, *J. Photochem. Photobiol., A 126*, 83−89.
58. Gouterman, M. (1978) Optical Spectra and Electronic Structure of Porphyrins and Related Rings, in *The Porphyrins* (Dolphin, D., Ed.) pp 1−165, Academic Press, New York.
59. Kim, D., Holten, D., and Gouterman, M. (1984) Evidence from Picosecond Transient Absorption and Kinetic Studies of Charge-Transfer States in Copper(II) Porphyrins, *J. Am. Chem. Soc. 106*, 2793−2798.
60. Cunningham, K. L., McNett, K. M., Pierce, R. A., Davis, K. A., Harris, H. H., Falck, D. M., and McMillin, D. R. (1997) EPR spectra, luminescence data, and radiationless decay processes of copper(II) porphyrins, *Inorg. Chem. 36*, 608−613.
61. Liu, F., Cunningham, K. L., Uphues, W., Fink, G. W., Schmolt, J., and McMillin, D. R. (1995) Luminescence Quenching of Copper(II) Porphyrins with Lewis Bases, *Inorg. Chem. 34*, 2015−2018.
62. Lugo-Ponce, P., and McMillin, D. R. (2000) DNA-binding studies of Cu(T4), a bulky cationic porphyrin, *Coord. Chem. Rev. 208*, 169−191.
63. Chen, L. X., Shaw, G. B., Liu, T., Jennings, G., and Attenkofer, K. (2004) Exciplex formation of copper(II) octaethylporphyrin revealed by pulsed X-rays, *Chem. Phys. 299*, 215−223.
64. Kruglik, S. G., Apanasevich, P. A., Chirvony, V. S., Kvach, V. V., and Orlovich, V. A. (1995) Resonance Raman, Cars, and Picosecond Absorption Spectroscopy of Copper Porphyrins: The Evidence for the Exciplex Formation with Oxygen-Containing Solvent Molecules, *J. Phys. Chem. 99*, 2978−2995.
65. Chirvony, V. S. (2003) Primary photoprocesses in cationic 5,10,-15,20-meso-tetrakis(4-N-methylpyridiniumyl)porphyrin and its transition metal complexes bound with nucleic acids, *J. Porphyrins Phthalocyanines 7*, 766−774.
66. Kruglik, S. G., Mojzes, P., Mizutani, Y., Kitagawa, T., and Turpin, P. Y. (2001) Time-resolved resonance raman study of the exciplex formed between excited Cu-porphyrin and DNA, *J. Phys. Chem. B 105*, 5018−5031.
67. Keating, L. R., and Szalai, V. A. (2004) Parallel-stranded guanine quadruplex interactions with a copper cationic porphyrin, *Biochemistry 43*, 15891−15900.
68. Muller, W., and Crothers, D. M. (1968) Studies of Binding of Actinomycin and Related Compounds to DNA, *J. Mol. Biol. 35*, 251−290.
69. Huang, X. F., Nakanishi, K., and Berova, N. (2000) Porphyrins and metalloporphyrins: Versatile circular dichroic reporter groups for structural studies, *Chirality 12*, 237−255.
70. Lewis, F. D. (2005) DNA molecular photonics, *Photochem. Photobiol. 81*, 65−72.
71. Balaz, M., Holmes, A. E., Benedetti, M., Rodriguez, P. C., Berova, N., Nakanishi, K., and Proni, G. (2005) Synthesis and circular dichroism of tetraarylporphyrin-oligonucleotide conjugates, *J. Am. Chem. Soc. 127*, 4172−4173.
72. Geacintov, N. E., Ibanez, V., Rougee, M., and Bensasson, R. V. (1987) Orientation and Linear Dichroism Characteristics of Porphyrin DNA Complexes, *Biochemistry 26*, 3087−3092.
73. Strickland, J. A., Banville, D. L., Wilson, W. D., and Marzilli, L. G. (1987) Metalloporphyrin Effects on Properties of DNA Polymers, *Inorg. Chem. 26*, 3398−3406.
74. Chirvony, V. S., Galievsky, V. A., Terekhov, S. N., Dzhagarov, B. M., Ermolenkov, V. V., and Turpin, P. Y. (1999) Binding of the Cationic 5-Coordinate Zn(II)-5,10,15,20-tetrakis(4-*N*-methylpyridyl)porphyrin to DNA and Model Polynucleotides: Ionic-Strength Dependent Intercalation in $[Poly(dG\text{-}dC)]_2$, *Biospectroscopy 5*, 302−312.
75. Whitten, D. G., Lopp, I. G., and Wildes, P. D. (1968) Fluorescence of Zinc and Magnesium Etioporphyrin. I. Quenching and Wavelength Shifts Due to Complex Formation, *J. Am. Chem. Soc. 90*, 7196−7200.
76. Kruglik, S. G., Galievsky, V. A., Chirvony, V. S., Apanasevich, P. A., Ermolenkov, V. V., Orlovich, V. A., Chinsky, L., and Turpin, P. Y. (1995) Dynamics and Mechanism of the Exciplex Formation between Cu(Tmpy-P4) and DNA Model Compounds Revealed by Time-Resolved Transient Absorption and Resonance Raman Spectroscopies, *J. Phys. Chem. 99*, 5732−5741.
77. Sari, M. A., Battioni, J. P., Mansuy, D., and Lepecq, J. B. (1986) Mode of Interaction and Apparent Binding Constants of Meso-Tetraaryl Porphyrins Bearing between One and Four Positive Charges with DNA, *Biochem. Biophys. Res. Commun. 141*, 643−649.
78. Berova, N., and Nakanishi, K. (2000) Exciton Chirality Method: Principles and Applications, in *Circular Dichroism: Principles and Applications* (Nakanishi, K., Berova, N., and Woody, R., Eds.) pp 337−382, Wiley-VCH, New York.
79. Armitage, B. A. (2006) DNA-Templated Assembly of Helical Multichromophore Aggregates, *Mol. Supramol. Photochem. 14*, 255−287.
80. Bloomfield, W. A., Crothers, D. M., and Tinoco, J., Jr. (2000) *Nucleic Acids: Structures, Properties, and Functions*, University Science, Sausalito, CA.
81. Calladine, C. R., and Drew, H. R. (1997) *Understanding DNA*, 2nd ed., Academic Press, New York.
82. Marzilli, L. G., Petho, G., Lin, M. F., Kim, M. S., and Dixon, D. W. (1992) Tentacle Porphyrins-DNA Interactions, *J. Am. Chem. Soc. 114*, 7575−7577.
83. Mukundan, N. E., Petho, G., Dixon, D. W., and Marzilli, L. G. (1995) DNA-Tentacle Porphyrin Interactions: AT Over GC Selectivity Exhibited by an Outside Binding Self-Stacking Porphyrin, *Inorg. Chem. 34*, 3677−3687.
84. Pasternack, R. F., Caccam, M., Keogh, B., Stephenson, T. A., Williams, A. P., and Gibbs, E. J. (1991) Long-Range Fluorescence Quenching of Ethidium Ion by Cationic Porphyrins in the Presence of DNA, *J. Am. Chem. Soc. 113*, 6835−6840.
85. Lincoln, P., Tuite, E., and Norden, B. (1997) Short-circuiting the molecular wire: Cooperative binding of Δ-$[Ru(phen)_2dppz]^{2+}$ and Δ-$[Rh(phi)_2bipy]^{3+}$ to DNA, *J. Am. Chem. Soc. 119*, 1454−1455.
86. Olson, E. J. C., Hu, D. H., Hormann, A., and Barbara, P. F. (1997) Quantitative modeling of DNA-mediated electron transfer between metallointercalators, *J. Phys. Chem. B 101*, 299−303.
87. Rodriguez, J., and Holten, D. (1990) Ultrafast Photodissociation of a Metalloporphyrin in the Condensed Phase, *J. Chem. Phys. 92*, 5944−5950.
88. Kruglik, S. G., Mizutani, Y., and Kitagawa, T. (1997) Time-resolved resonance Raman study of the primary photoprocesses of nickel(II) octaethylporphyrin in solution, *Chem. Phys. Lett. 266*, 283−289.

BI700293G